

Signature of the Converging Inflow into Black Hole: Observational Evidence of a Black Hole Existence

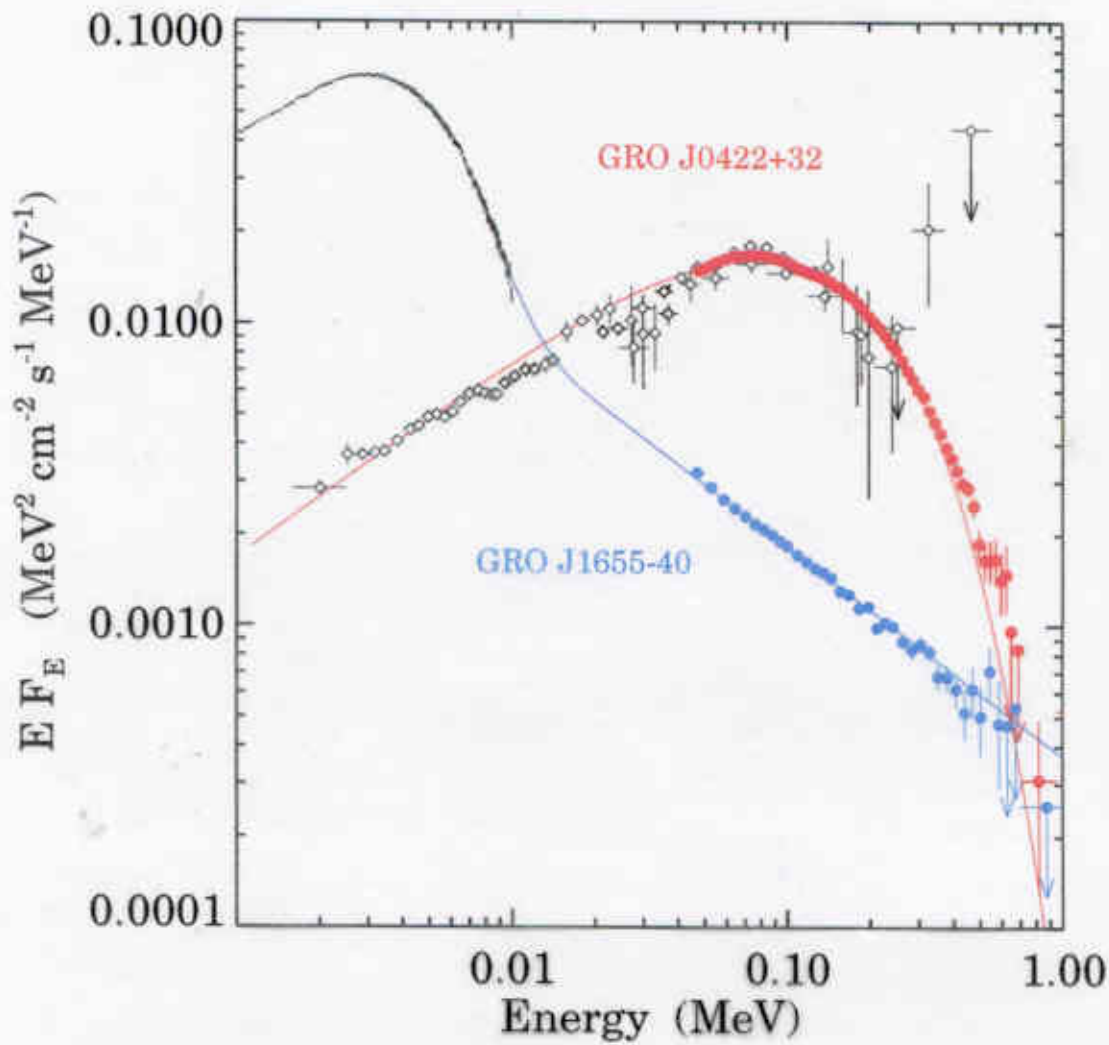
Lev Titarchuk (GMU/NRL/GSFC)

In collaboration with:

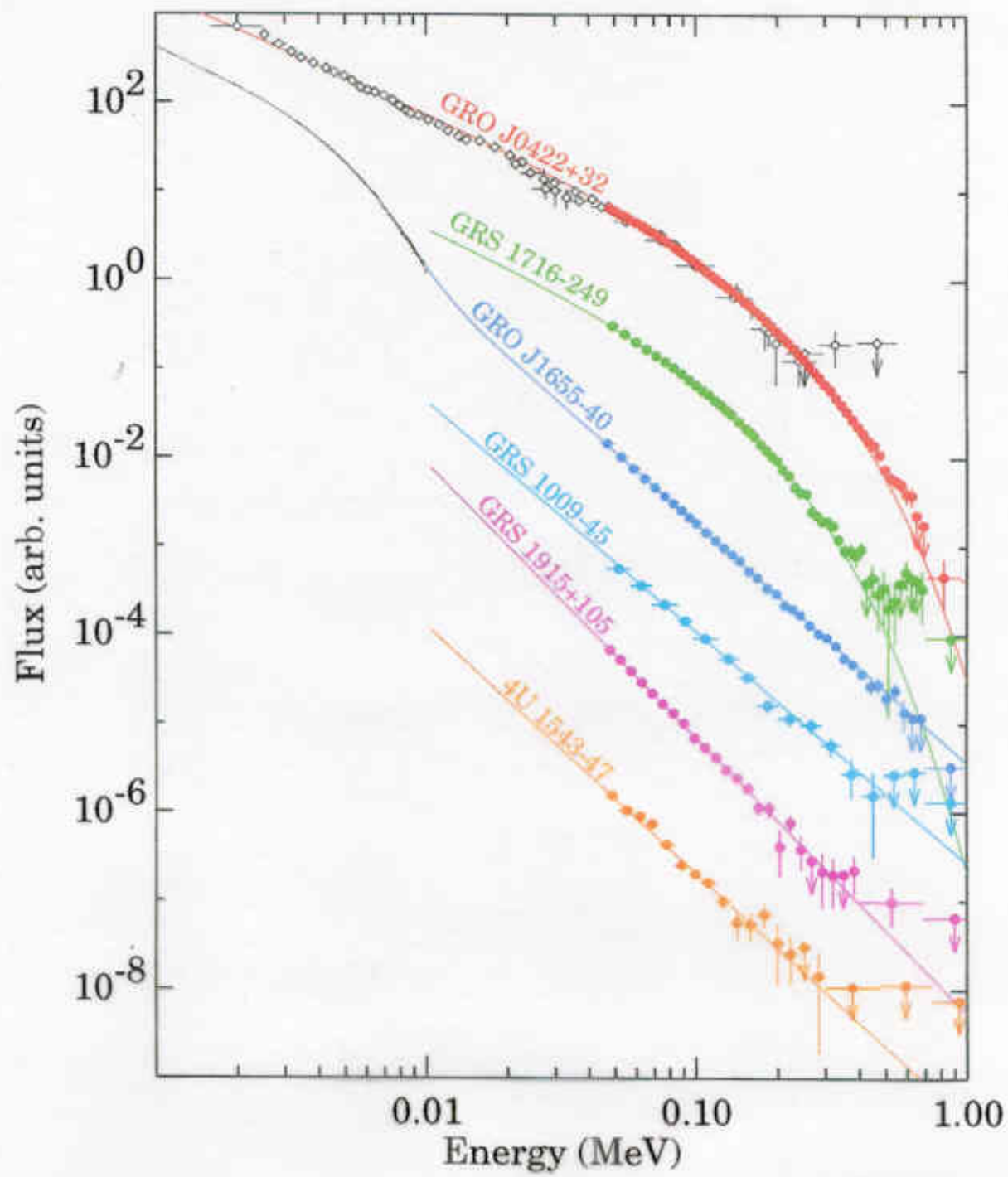
P. Laurent¹

¹ Center d'Etudes de Saclay, CEA

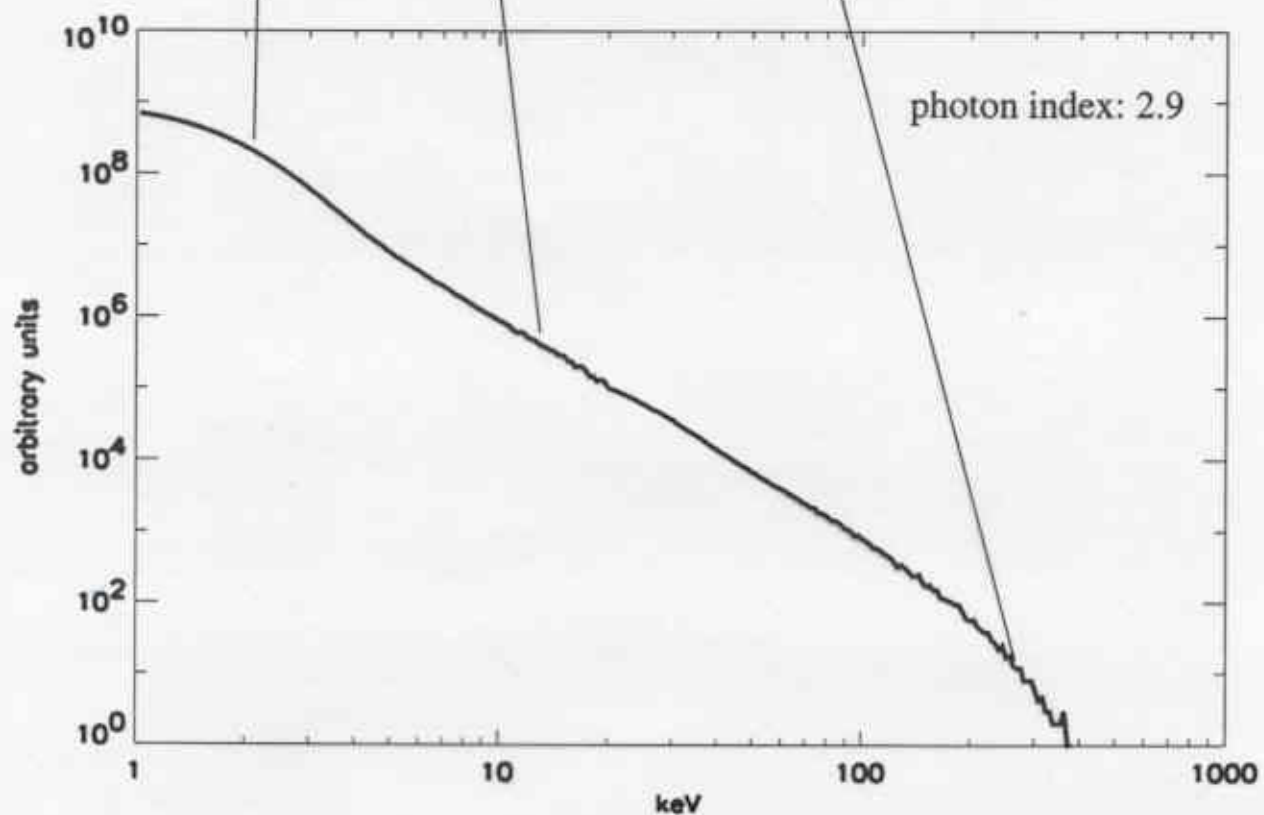
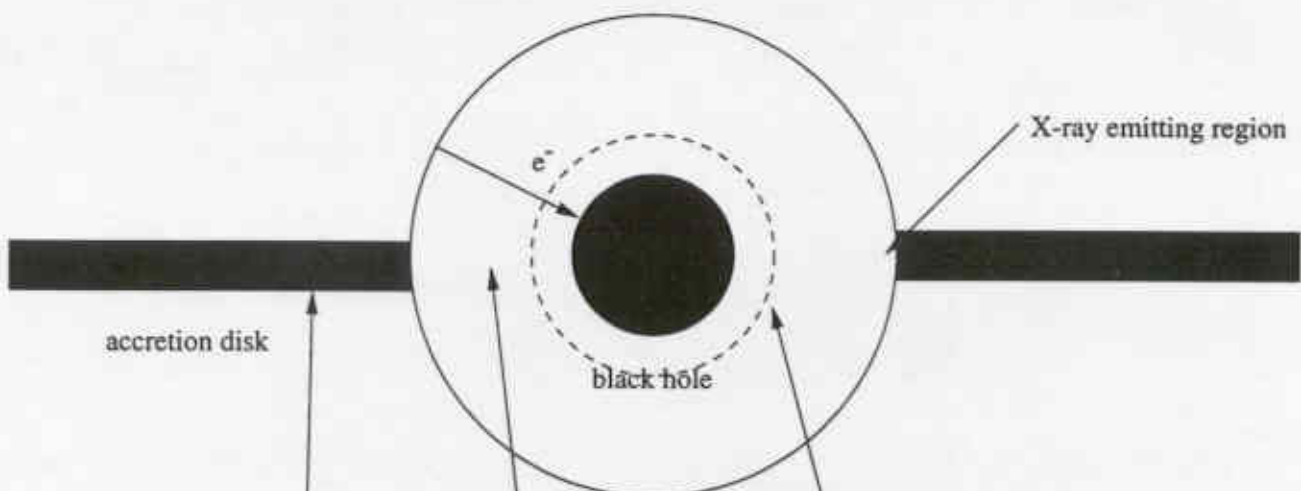
Spectral State Transition in Black Hole Candidates Binaries



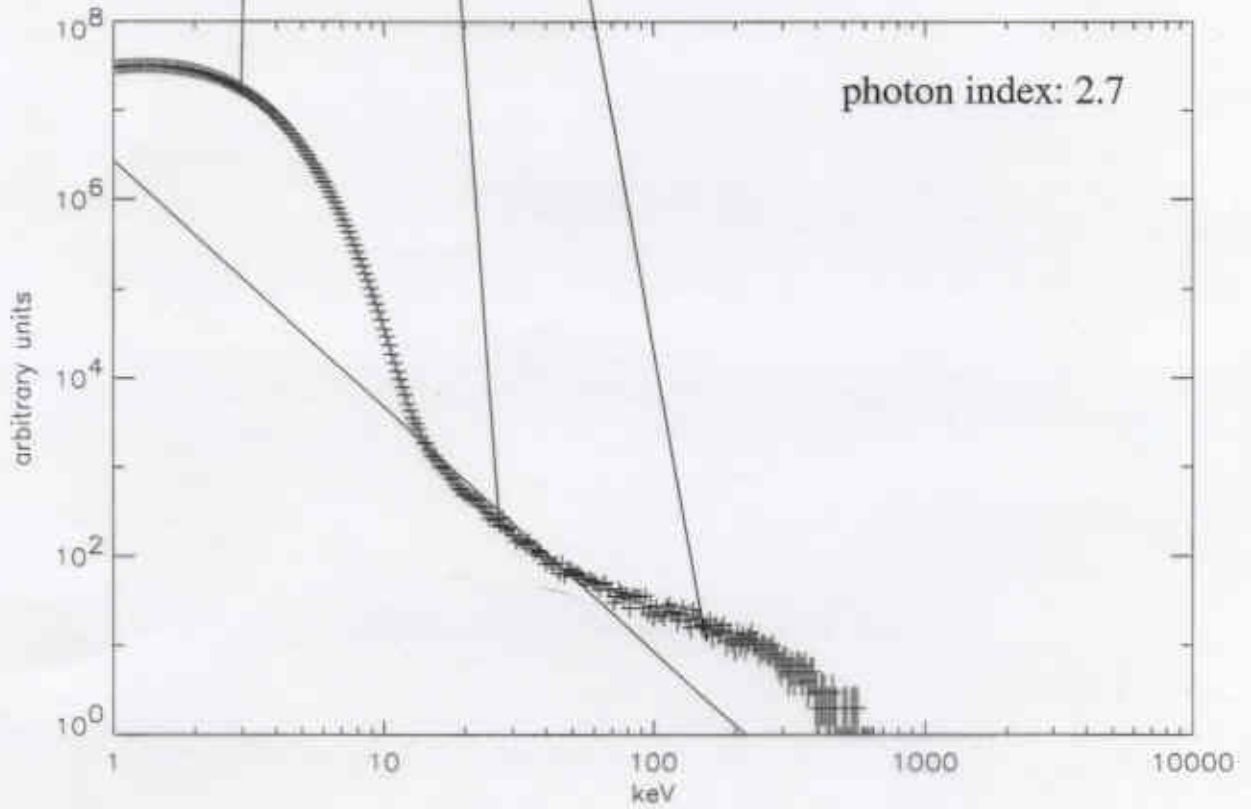
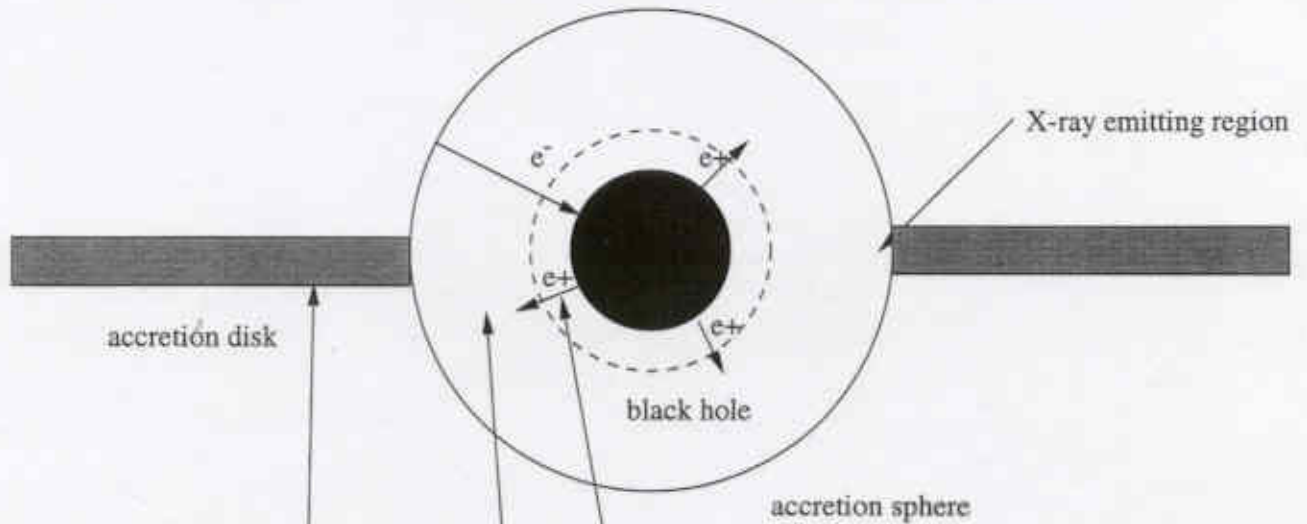
Grove et al. (1998)



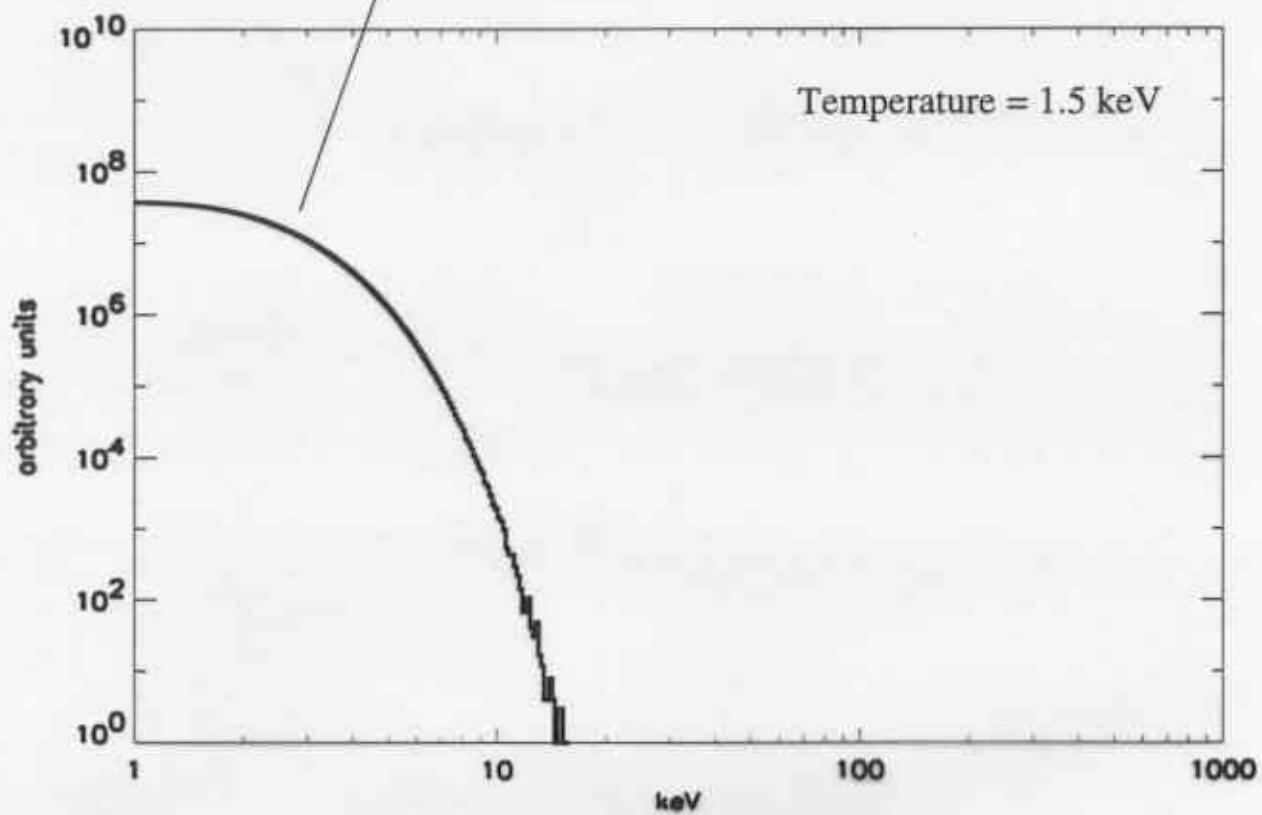
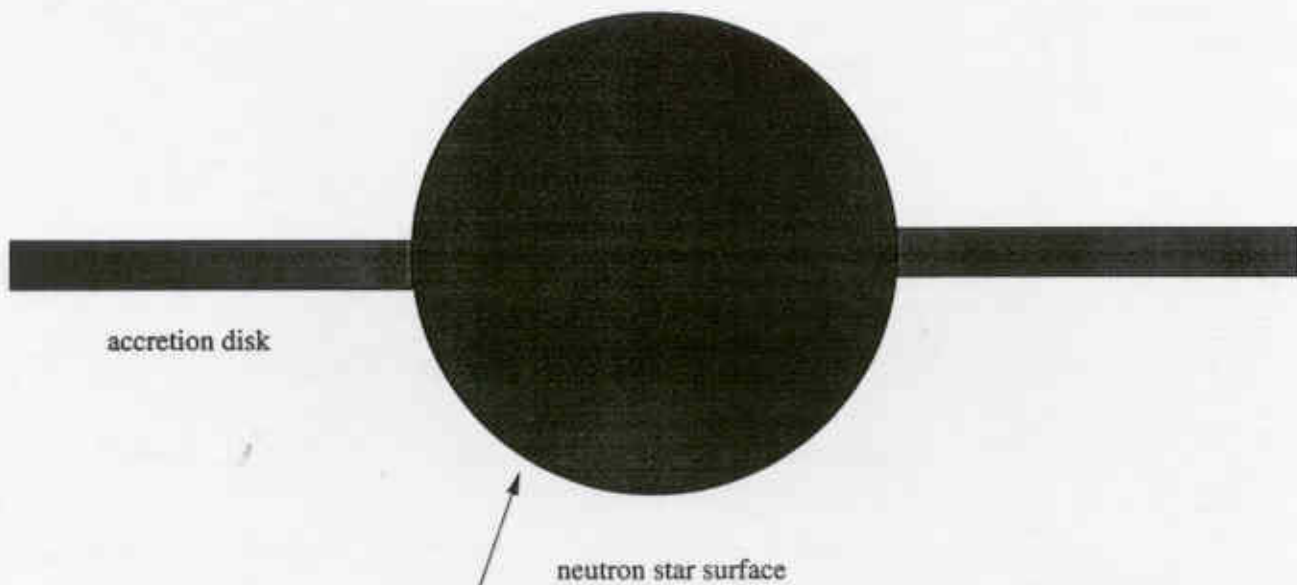
HIGH STATE OF BLACK HOLE SYSTEM



X-RAY SPECTRAL FORMATION AND PAIR CREATION AS BLACK HOLE SIGNATURES



HIGH STATE OF NEUTRON STAR SYSTEM



Scattering events in the converging flow

accretion flow



$$\frac{v'}{v} = \frac{1 - \mu_1 \beta}{1 - \mu_2 \beta} \quad (\text{Doppler effect})$$

$$\mu_1 = \vec{n}_1 \cdot \vec{v} / v \quad \text{and} \quad \mu_2 = \vec{n}_2 \cdot \vec{v} / v$$

For highly relativistic speeds,
 $v \rightarrow c$ ($\gamma \gg 1$)

$$\theta_2 \approx \arccos \mu \approx \frac{1}{\gamma} \quad \text{and} \quad \frac{v'}{v} = (1 - \mu_1) 2\gamma^2$$



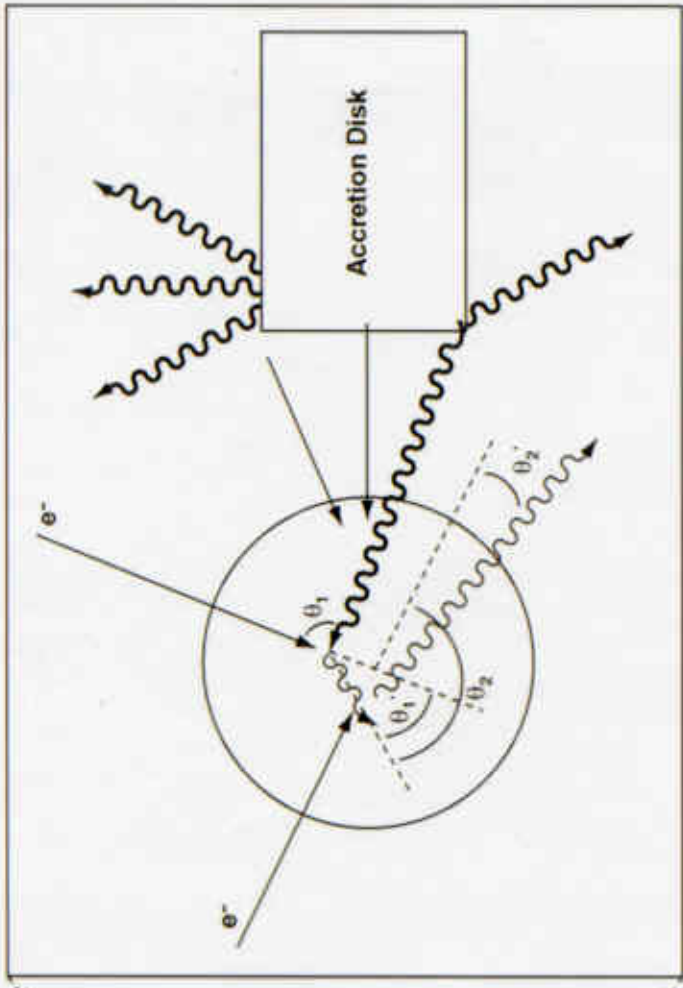
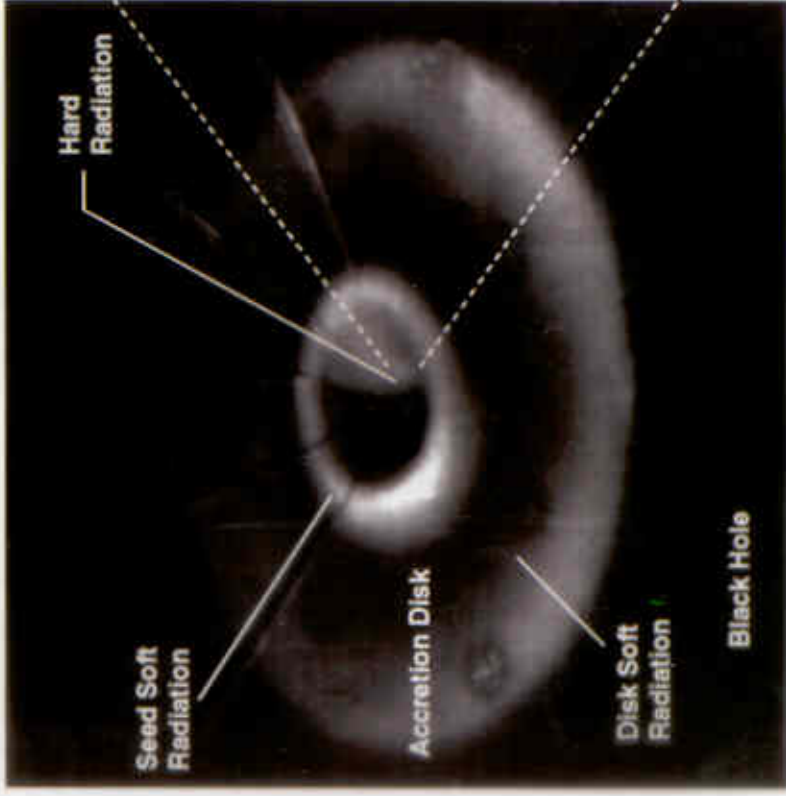
In the nonrelativistic limit

$$\frac{v'}{v} = 1 + (\mu_2 - \mu_1)\beta + (\mu_2\beta)^2$$

for $\mu_2 \sim 1$ and $\beta > 0$

the photon energy change per scattering,

$$0 < \frac{\delta v}{v} \sim \frac{dv}{v} ; \quad \text{because } \frac{dv}{v} > 0.$$



Observer

Spectral index of the converging inflow spectrum

- Main idea of the power law formation:

$$I_\nu \propto \nu^k,$$

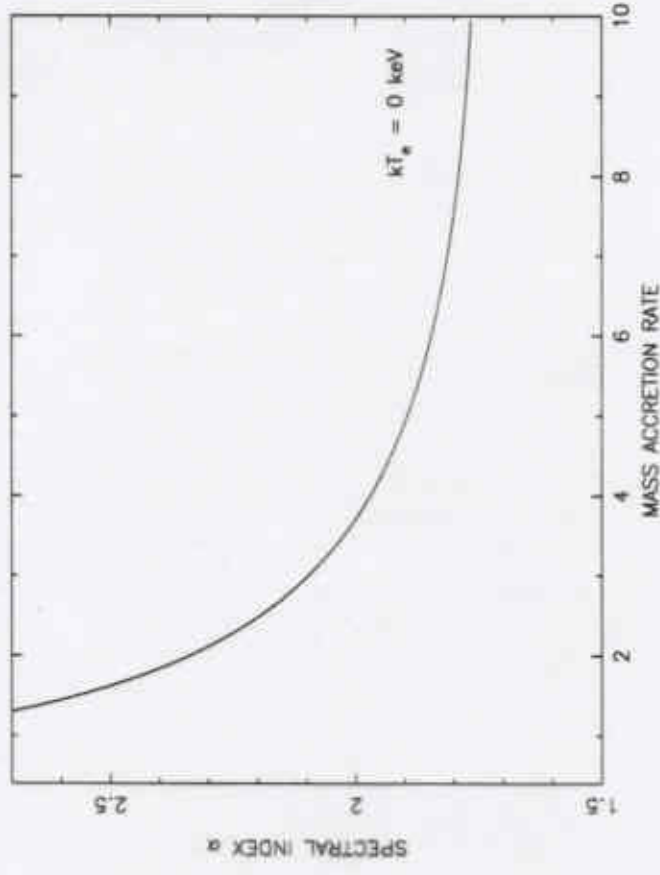
where p is a probability of single scattering.

$$\nu / \nu_0 = 1 + \eta,$$

after k scatterings

$$\nu_k / \nu_0 = (1 + \eta)^k.$$

Thus $I = (\nu / \nu_0)^{-\alpha}$ where $\alpha = \ln(1/p) / \ln(1 + \eta)$



FORMULATION AND SOLUTION OF THE PROBLEM

The Full Relativistic Treatment

- The line element for the Schwarzschild black hole:

$$ds^2 = -f dt^2 + \frac{dr^2}{f} + r^2 d\Omega^2 \quad (4)$$

$f = 1 - r_s/r$, $r_s = 2GM/c^2$, and t, r, θ, φ are the event coordinates with $d\Omega^2 = d\theta^2 + \sin^2 \theta d\varphi^2$.

- The full relativistic equation for the occupation number $N(x, p)$ (Lindquist 1966, see also T& Zannias 1998):

$$\begin{aligned} & \mu\sqrt{f}\frac{\partial N}{\partial r} - \nu\mu\frac{\partial\sqrt{f}}{\partial r}\frac{\partial N}{\partial\nu} \\ & - (1 - \mu^2) \left(\frac{\partial\sqrt{f}}{\partial r} - \frac{\sqrt{f}}{r} \right) \cdot \frac{\partial N}{\partial\mu} = \int_0^\infty d\nu_1 \int_{4\pi} d\Omega_1 \\ & \left[\left(\frac{\nu_1}{\nu} \right)^2 \sigma_s(\nu_1, \nu, \xi) N(\nu_1, \mu_1) - \sigma_s(\nu, \nu_1, \xi) N(\nu, \mu) \right] \end{aligned} \quad (5)$$

The scattering kernel σ_s being given by:

$$\begin{aligned} \sigma_s(\nu \rightarrow \nu_1, \xi) &= \frac{3}{16\pi} \frac{n_e \sigma_T}{\nu z} \int_0^\pi \sin\theta d\theta \int d^3\mathbf{v} \\ & \frac{F(\mathbf{r}, \mathbf{P}_e)}{\gamma} \left\{ 1 + \left[1 - \frac{1 - \xi}{\gamma^2 D D'} \right]^2 + \frac{z z' (1 - \xi)^2}{\gamma^2 D D'} \right\} \\ & \times \delta(\xi - 1 + \gamma D'/z - \gamma D/z'), \end{aligned} \quad (6)$$

$z = h\nu/m_e c^2$, $D = 1 - \mu V$, $D_1 = 1 - \mu' V$, $\gamma = (1 - V^2)^{-1/2}$, $\xi = \Omega' \cdot \Omega$ is the cosine of scattering angle and $F(\mathbf{r}, \mathbf{P}_e)$ stands for the local Maxwellian distribution.

ANALYTICAL SOLUTION OF THE PROBLEM

- The Green's function for the low-energy photon injection.
- The power-law part of the spectrum occurs at energies lower than that of Wien cut-off
- Let us to seek the solution in the form

$$N(\mathbf{r}, \nu, \Omega) = \nu^{-3+\alpha} \mathbf{J}(\mathbf{r}, \mu). \quad (7)$$

We get from (5) that

$$\begin{aligned} \ell \mathbf{J} &= \mu \sqrt{f} \frac{\partial \mathbf{J}}{\partial \mathbf{r}} + (\alpha + 3) \mu \frac{\partial \sqrt{f}}{\partial \mathbf{r}} \mathbf{J} \\ &\quad - (1 - \mu^2) \left(\frac{\partial \sqrt{f}}{\partial \mathbf{r}} - \frac{\sqrt{f}}{\mathbf{r}} \right) \frac{\partial \mathbf{J}}{\partial \mu} \\ &= n_e \sigma_T \left[-\mathbf{J} + \frac{1}{4\pi} \int_{-1}^1 d\mu_1 \int_0^{2\pi} d\varphi \mathbf{R}(\xi) \mathbf{J}(\mu_1, \tau) \right], \end{aligned} \quad (8)$$

$$\begin{aligned} \mathbf{R}(\xi) &= \frac{3}{4} \int_0^\pi \sin \theta d\theta \int d^3 \mathbf{v} \frac{\mathbf{F}(\mathbf{r}, \mathbf{P}_e)}{\gamma^2} \\ &\quad \times \left(\frac{\mathbf{D}_1}{\mathbf{D}} \right)^{\alpha+2} \frac{1}{\mathbf{D}_1} [1 + (\xi')^2], \end{aligned} \quad (9)$$

where ξ' is the cosine of scattering angle.

- The whole problem is reduced to the eigenvalue problem for equation (8).
- There are two boundary conditions that our solution satisfy. 1) there is no scattered radiation outside of the atmosphere. 2) that we have an absorptive boundary at the BH horizon radius, r_s . Namely, there is no radiation which emerges from the horizon.

Photon Trajectories in the Curve Space

- The differential equation for the characteristics of the operator ℓ :

$$\left[-\frac{1}{2x^2(1-x^{-1})} + x^{-1} \right] dx = d[\ln(1-\mu^2)^{-1/2}], \quad (10)$$

where $x = r/r_s$ is a dimensionless radius.

- The integral curves (the characteristic curves):

$$\frac{x(1-\mu^2)^{1/2}}{(1-x^{-1})^{1/2}} = \frac{x_0(1-\mu_0^2)^{1/2}}{(1-x_0^{-1})^{1/2}} = p, \quad (11)$$

where p is an impact parameter.

In the the flat geometry, the characteristics are just straight lines

$$x(1-\mu^2)^{1/2} = p, \quad (12)$$

where the impact parameter p is the distance of a given straight line to the center.

One can resolve equation (11) with respect of μ to get

$$\mu = \pm(1-p^2/y^2)^{1/2} \quad (13)$$

where $y = x^{3/2}/(x-1)^{1/2}$.

This iteration formalism is identical to the integral-equation formalism in which

$$B^0(r, \mu) = \sum_{i=0}^n C_i P_i(\mu) B_i^0(r), \quad (28)$$

where the set of $B_i^0(r)$ components of the source function, $B(r, \Omega)$, is determined by the system of the integral equations (compare with TL95):

$$B_i^0(r) = \frac{1}{2} \sum_{j=0}^n C_j \left[\int_{-1}^0 p(\mu') p_j(\mu') d\mu' \int_0^{T(r_{\text{bn}}, r, \mu')} \right. \\ \times \exp \{-T[r_{\text{bn}}, r'(r, \mu'), \mu']\} B_j^0(r') dT + \int_0^1 p(\mu') p_j(\mu') d\mu' \\ \times \left. \int_0^{T(r_{\text{bn}}, r, \mu')} \exp \{-T[r_{\text{bn}}, r'(r, \mu'), \mu']\} B_j^0(r') dT \right]. \quad (29)$$

Thus the eigenvalue problem (eqs. [21]–[24b]) can be reduced to an eigenproblem for a system of integral equations (eq. [29]) where the optical paths, $T(r_{\text{bn}}, r, \mu)$, and the expansion coefficients of the phase function, C_i , depend on the spectral index, α , as a parameter. In other words, one has to find the values of α that guarantee the existence of the nontrivial solution of equation (29). In § 3.2 and Appendix B, we shall proceed with the numerical solution of the eigenvalue problem by presenting the bulk motion phase function, $R_b(\xi_s)$, in the degenerated form (see eq. [26]).

Now it is worth noting that in the case of the pure thermal motion in the isothermal plasma cloud, the problem is substantially simplified. The source function, $B^0(r, \mu)$, can be replaced by its zeroth moment, $B_0^0(r)$ (TL95), which guarantees the accuracy of the spectral index determination to better than 10% in the worst cases (Giesler & Kirk 1997).

For example, the equation for the zeroth moment, $B_0^0(r)$, reads

$$B_0^0(r) = \frac{C_0}{2} \left[\int_{-1}^0 d\mu' \int_0^{T(r_{\text{bn}}, r, \mu')} \right. \\ \times \exp \{-T[r_{\text{bn}}, r'(r, \mu'), \mu']\} B_0^0(r') dT + \int_0^1 d\mu' \\ \times \left. \int_0^{T(r_{\text{bn}}, r, \mu')} \exp \{-T[r_{\text{bn}}, r'(r, \mu'), \mu']\} B_0^0(r') dT \right], \quad (30)$$

where C_0 is the zero-moment of the phase function.

3.2. Photon Trajectories and the Characteristics of the Space Operator, ℓ

The characteristics of the differential operator, ℓ , are determined by the following differential equation:

$$\left[-\frac{1}{2x^2(1-x^{-1})} + x^{-1} \right] dx = d[\ln(1-\mu^2)^{-1/2}], \quad (31)$$

where $x = r/r_s$ is a dimensionless radius. The integral curves of this equation (the characteristic curves) are given by

$$\frac{x(1-\mu^2)^{1/2}}{(1-x^{-1})^{1/2}} = \frac{x_0(1-\mu_0^2)^{1/2}}{(1-x_0^{-1})^{1/2}} = p, \quad (32)$$

where p is an impact parameter at infinity; p can also be determined at a given point in a characteristic by the cosine of an angle between the tangent to and the radius vector to the point and by the given point position, x_0 .

In the flat geometry, the characteristics are just straight lines:

$$x(1-\mu^2)^{1/2} = p, \quad (33)$$

where an impact parameter, p , is the distance from a given point to the center.

We can resolve equation (32) with respect to μ to get

$$\mu = \pm(1-p^2/y^2)^{1/2}, \quad (34)$$

where $y = x^{3/2}/(x-1)^{1/2}$. The graph of y as a function of x is presented in Figure 1, which allows us to comprehend the possible range of radii for the given impact parameter, p , through the inequality $p \leq y$. For example, if $p \leq (6.75)^{1/2}$, then the photon can escape from the inner boundary (the black hole horizon) toward the observer or vice versa; all photons going toward the horizon having these impact parameters are gravitationally attracted by the black hole. However, if $p > (6.75)^{1/2}$, then the finite trajectories are possible with the radius range between $1 \leq x \leq 1.5$ or the infinite trajectories with $p \leq y(x)$ (x is always more than 1.5).

3.3. Spectral Index Determination

We are assuming a free fall for the background flow, where the bulk velocity of the infalling plasma is given by $v(r) = c(r_s/r)^{1/2}$. In the kinetic equations (eqs. [12] and [16]), the density, n , is measured in the local rest frame of the flow, and it is $n = \dot{m}(r_s/r)^{1/2}/(2r\sigma_T)$. Here $\dot{m} = M/M_g$, M is the

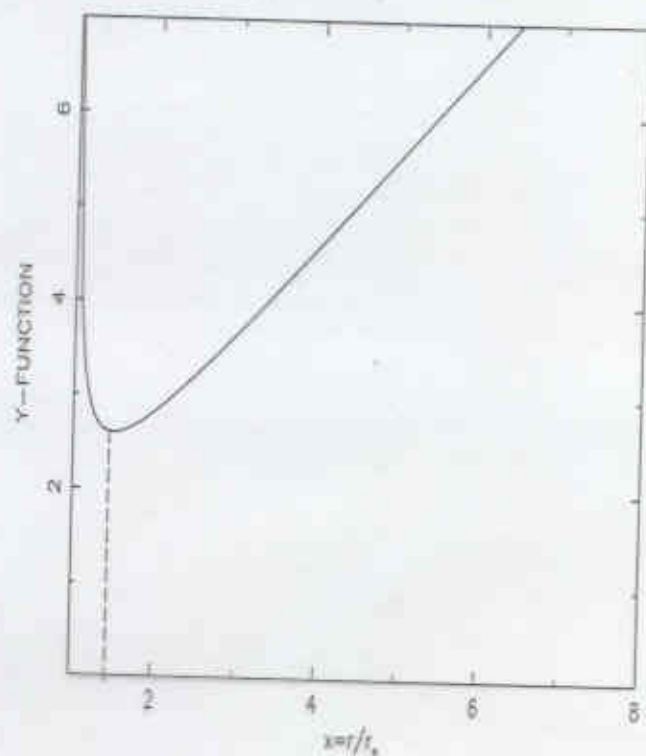


FIG. 1.—Plot of the photon trajectory phase space: the phase-space function, y , vs. the dimensionless radius, $x = r/r_s$.

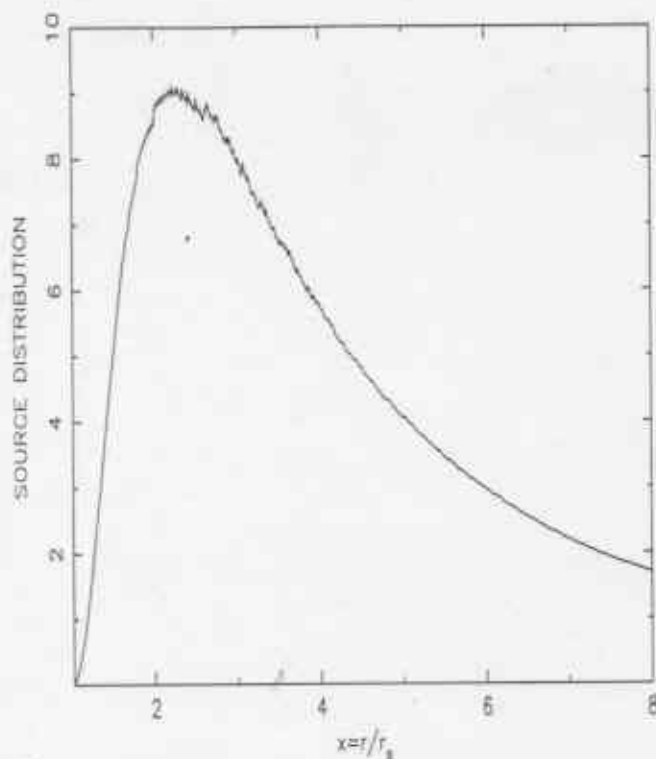


FIG. 3.—Plot of the source function distribution, eq. (B1), in arbitrary units vs. the dimensionless radius, $x = r/r_g$, for the dimensionless mass accretion rate, $\dot{m} = 4$, and $\mu = 0$.

by upscattering of the soft photons off the converging electrons.

Our calculations were made under the assumption of the free fall velocity profile. Since the energy gain due to the bulk motion Comptonization is not bigger than a factor 3 (if the spectral indices are higher than 1.5; TMK97), it follows that we can safely neglect the effects of the radiation force in our calculations if the injected photon flux in the converging inflow is of order of a few percent of the Eddington luminosity.

The assumption of Thomson scattering accepted in our solution restricts the relevant energy range to $E < m_e c^2$.

Our approach cannot determine accurately the exact position of the high-energy cutoff that is formed owing to the downscattering of the very energetic photons in the bulk motion electron atmosphere. Additional efforts are required to confirm the qualitative estimates of the high-energy cutoff position as being of order $m_e c^2$ (TMK97). Laurent & Titarchuk (1998), by using Monte Carlo calculations, checked and confirmed these results for the spectral indices and the TMK97 estimates of the high-energy cutoff position.

As a conclusion, we would like to point out the definitive (according to our model) difference between black holes and neutron stars, as can be ascertained in their spectral properties while in their soft states, when their luminosity is dominated by the quasi-thermal, soft, component: in the black hole case, there should always be an additional steep power-law high-energy tail extending to energies $\sim m_e c^2$. This component should be absent in neutron star systems because the effect of the bulk motion is suppressed by the radiation pressure in this case.

We presented the full relativistic formalism and solved semianalytically the kinetic equation by using the TL95 eigenfunction method (see also Giesler & Kirk 1997) in the case of plasma infalling radially into a compact object with a soft source of input photons. We found that *the converging flow has crucial effects on the emergent spectrum for moderately super-Eddington mass accretion rates.*

Our power-law spectra can be applicable for the explanation of the observational situations in black hole candidate sources.

We thank the anonymous referee for reading and evaluating the present paper. L. T. would like to acknowledge support from NASA grants NCC 5-52 and NAG 5-3408 and Alex Muslimov and Leonid Ozernoy for discussions and useful suggestions. L. T. also acknowledges Wan Chen for pointing out some particular details of the observational situations in black hole candidate sources. The research of T. Z. is supported by Conacyt-Mexico through a Cathedral Partimonial Fellowship as well as by research funds from the University of Michoacana SNH through a grant from Coordinacion Cientifica.

APPENDIX A

GENERAL RELATIVISTIC RADIATIVE KINETIC FORMALISM

Let u be an arbitrary timelike unit vector ($u \cdot u \equiv u^\alpha u_\alpha = -1$, $u^0 > 0$) at some given spacetime point, x , and let $d_1 x$, $d_2 x$, $d_3 x$ be the three arbitrary displacement vectors (with components $d_1 x^i$, etc.) that span an element of hypersurface orthogonal to u . By using orthogonality of two vectors, u_i and

$$d\Sigma_i = \sqrt{(-g)\epsilon_{i\alpha\beta\gamma}} d_1 x^\alpha d_2 x^\beta d_3 x^\gamma, \quad (\text{A1})$$

to the element of the hypersurface, one can get the invariant volume element orthogonal to the unit vector, u , as follows:

$$dV = \sqrt{(-g)\epsilon_{i\alpha\beta\gamma}} u^i d_1 x^\alpha d_2 x^\beta d_3 x^\gamma, \quad (\text{A2})$$

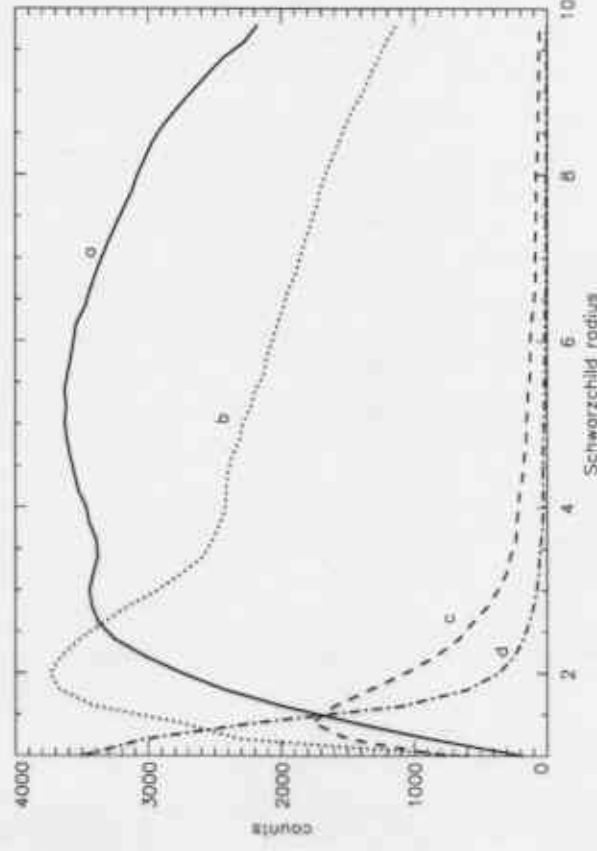
where $g = \det g_{\alpha\beta}$, $g_{\alpha\beta}$ is the metric tensor (see eq. [1]) and $\epsilon_{i\alpha\beta\gamma}$ is the Levi-Civita alternating symbol, $\epsilon_{0123} = +1$. Since N is independent of u , we may orient dV to make $u^0 = 1$, $u^i = 0$. Thus, in a local Minkowski frame it would be

$$dV = d^3 x. \quad (\text{A3})$$

Source Photon Spatial Distribution in CI Atmosphere

Our Monte Carlo simulations (Laurent & T 2001) reproduce the source function spatial distribution: 2-5 keV (curve a), 5-13 keV (curve b), 19-29 keV (curve c), and 60-150 keV (curve d).

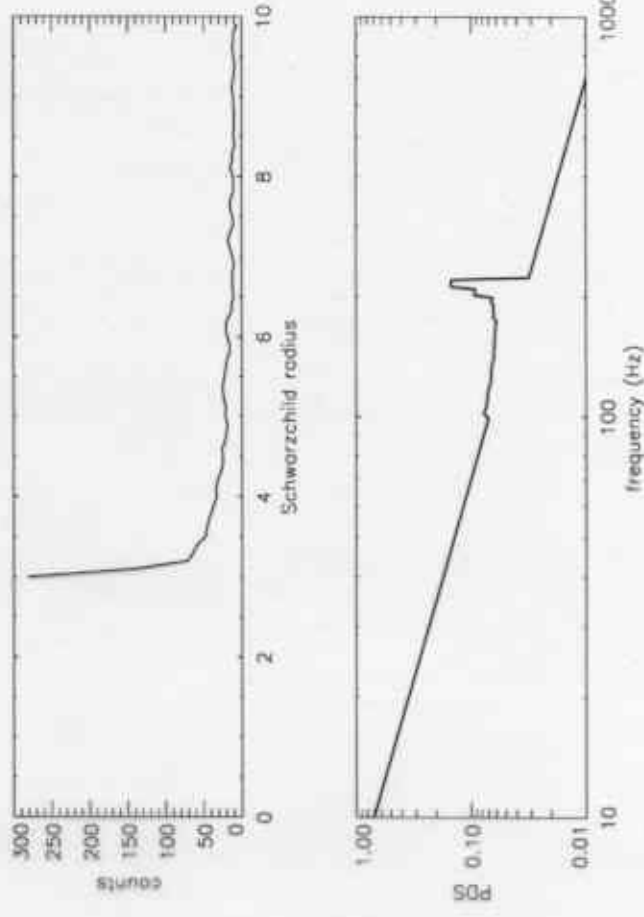
- We confirm the analytical results that the density of the highest energy X-ray photons is concentrated near the BH horizon.



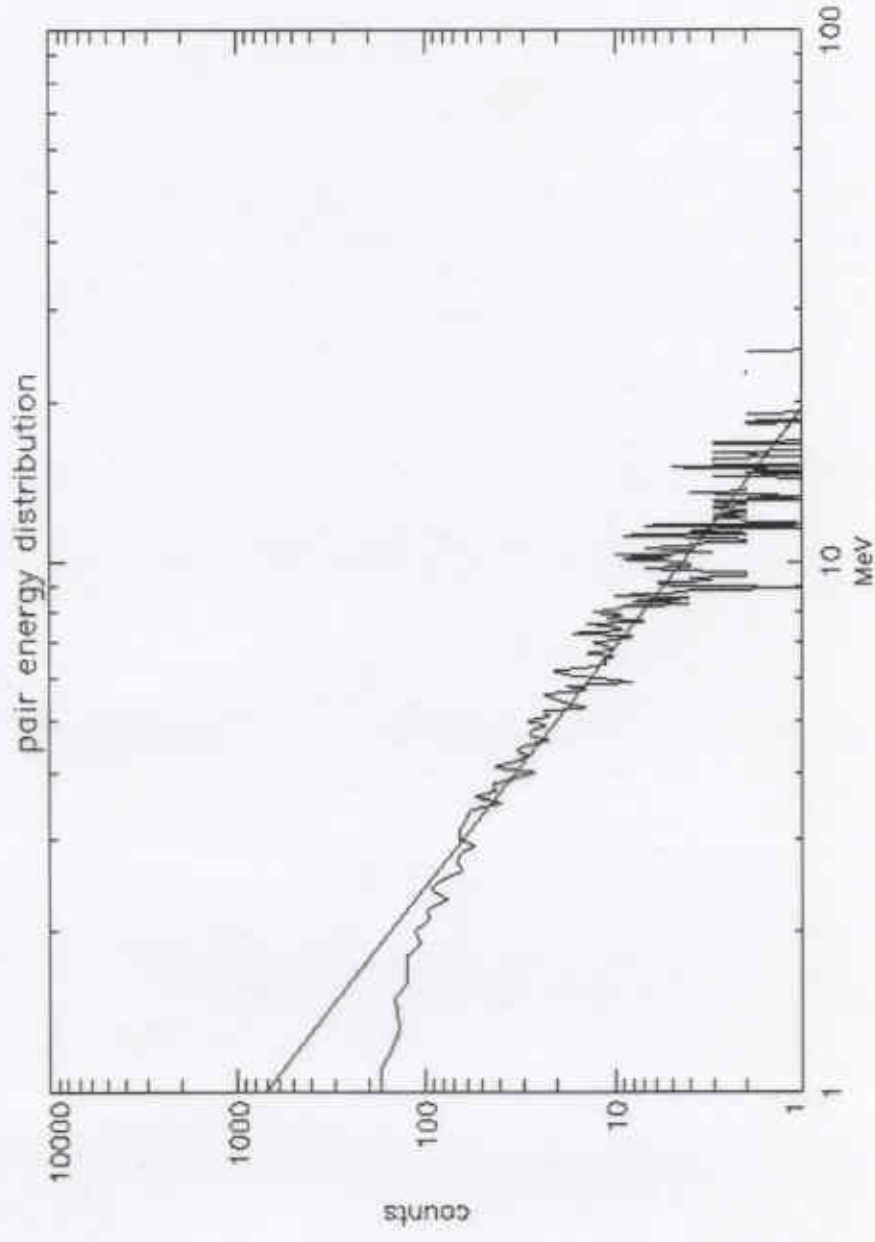
BH QPO feature

Upper panel: Distribution of soft photons over disk radius, which upscatters to energies 10 keV and higher in the atmosphere. *Lower panel:* PDS for photon energies higher than 10 keV. It is assumed that any disk annulus oscillates with Keplerian frequency (Laurent & T 2001).

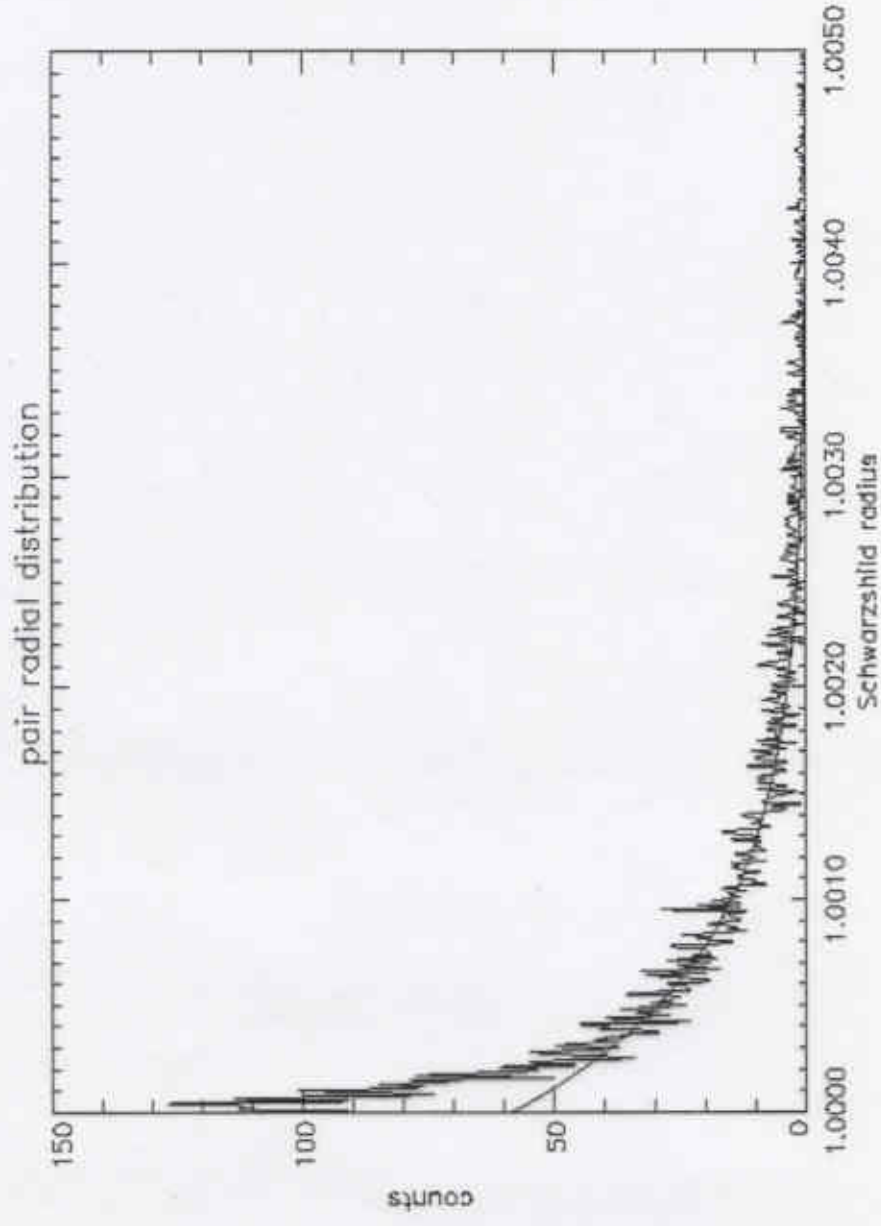
- **There is a striking similarity between the QPO frequency of the MC results and real observation of BH.**



Pair production as a signature of black hole : pair energy distribution



Pair production as a signature of black hole : pair radial distribution



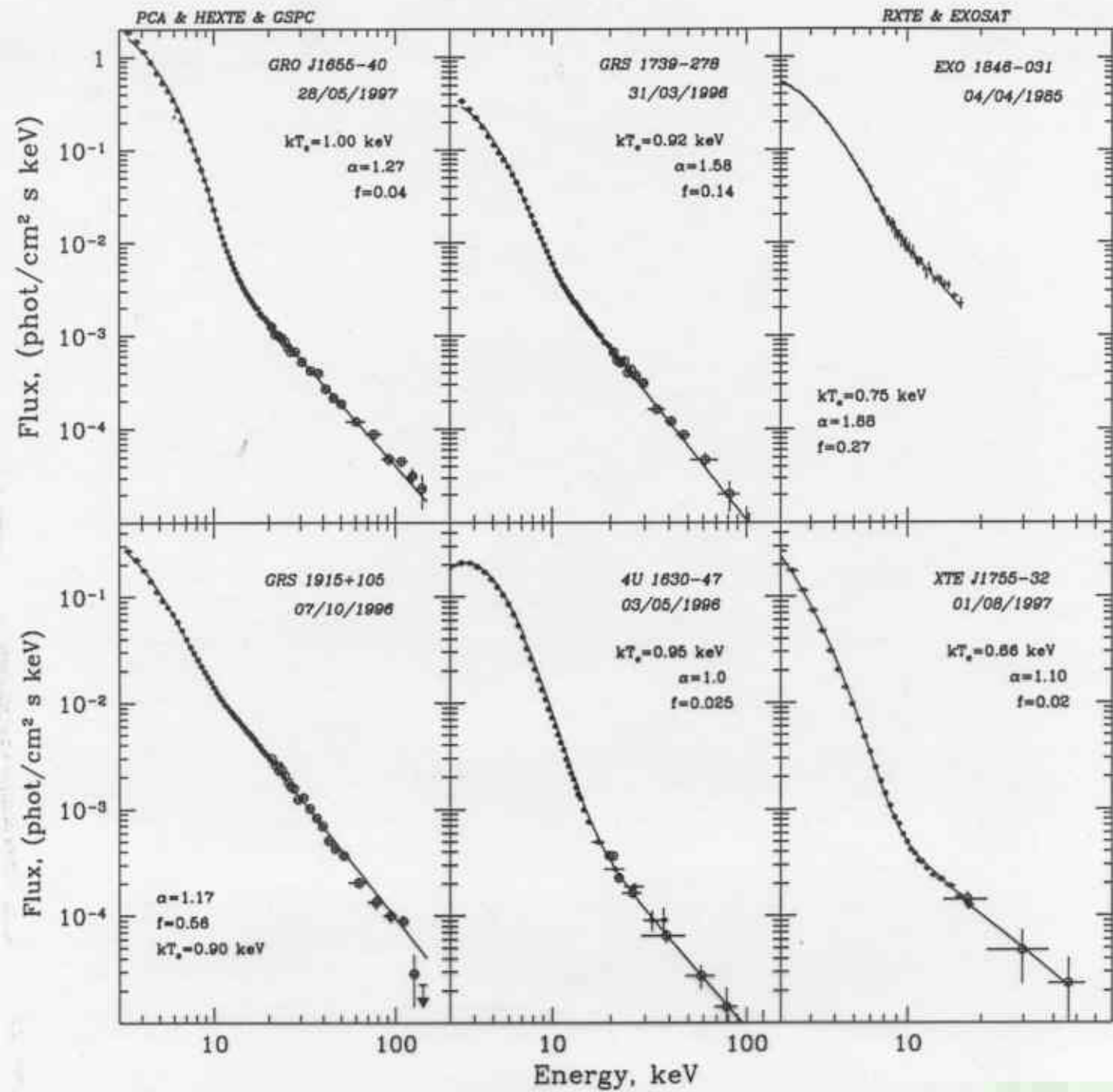


Fig. 1

CONCLUSIONS

- We have demonstrated through the analytical solution and Monte-Carlo simulations that the spectrum of the converging inflow into a black hole has a distinct feature in term of the shape. The spectrum in the low energy part has a blackbody like component and at high energies is a power law which extends to the energies of the order of the electron rest mass, 300 – 500 keV
- The power law spectral index goes to the asymptotic value 1.7, with an increase of the mass accretion rate in the converging inflow.
- This spectral feature should not be seen in NS binaries. The high radiation pressure almost stops the converging inflow when the mass accretion is near critical.
- The converging inflow feature is not seen in the hard state of the BH binaries. The hot Compton cloud prevents to detect the X-ray radiation from the BH vicinity.
- At the high accretion rate the tall standing wave is presumably formed in disk coming very close to the inner edge. Consequently, the oscillations of the disk soft photons modulated with the Keplerian frequency $\nu_K \sim 2$ kHz/m would cause the oscillations of the hard photon flux forming within the converging flow zone.

CONCLUSIONS

- Photon bending is an unavoidable effect near BH horizon ($1-3R_s$).
- Pairs are effectively produced by BHs due to the strong photon bending which leads to high compactness near a BH horizon.
- Doppler boosting of photons near BH in the pair outflow results in the extension of the converging inflow spectrum to energies of a few MeV